

Dynamics Analysis of a Three-Motor-Driven Scraper Conveyor

Zhengkun PEI¹, Qiang ZHANG, Jingru BAI

Shandong University of Science and Technology, Qianwangang Road 579, Qingdao, 266590, China.

Abstract. In response to the considerable fluctuations in motor load observed in traditional scraper conveyors employing dual-motor propulsion at both the machine's head and tail, we propose a novel three-motor drive configuration tailored explicitly for scraper conveyor systems. Leveraging the SGZ1200/2100 model scraper conveyor as our focal point and considering real-world operating conditions, we have engineered and assessed the dynamic simulation models for both dual-motor and three-motor driven structure. This thorough analysis has yielded torque characteristic curves for each motor within both configurations under both zero-load and full-load conditions. Our findings unequivocally demonstrate that the scraper conveyor employing the three-motor drive configuration excels in mitigating torque fluctuations at the machine's tail sprocket. This innovative design effectively minimizes torque differentials among adjacent motors, thereby furnishing invaluable data points for advancing research into the domain of multi-motor-driven scraper conveyor systems. This study serves as a promising stepping stone for future investigations in this burgeoning field of study.

Keywords. Scraper conveyor; Multi-point drive; Three-point drive; dynamics simulation

1. Introduction

Scraper conveyors, being the primary transportation equipment in underground coal mining operations, play crucial roles such as coal transport, coal mining machine guidance, and support for hydraulic advancements. The future of underground mining is moving toward greater safety, intelligence, efficiency, and environmental sustainability.

Currently, most mining scraper conveyors use a dual-drive structure at the head and tail. Dolipski, et al. ^[1-3] recorded in detail the uneven distribution of load on a single drive motor during the actual operation of the scraper conveyor. They also introduced the load distribution coefficient to represent the uneven distribution of load. Świder, et al. ^[4-6] analyzed the causes of uneven load under the starting condition of the scraper conveyor on the basis of the average current of the scraper conveyor motor. In actual working conditions, many scraper conveyors need to start under a load. Heavy load starts or prolonged operations may lead to overload and potential motor damage.

Moreover, with the dual-drive setup, where motors are situated at both ends, and each motor operates under differing power requirements, significant differences in the

¹ Corresponding Author: Zhengkun PEI, Shandong University of Science and Technology, e-mail address: 1063367212@qq.com.

linear velocities of the head and tail sprockets become apparent^[7]. This results in an increasing chain tension, making the chain more susceptible to failure, ultimately affecting the stability of the mining face.

To address the aforementioned challenges, our team proposed a novel multi-point drive system for the scraper conveyor. This involves adding multiple drive units as needed, as illustrated in Figure 1 (depicting the overall model of a five-point drive scraper conveyor). In this simulation, based on the actual working conditions of the SGZ1200/2100 scraper conveyor, equivalent models for two-point and three-point drive chain transmission systems were established. Dynamic simulations were conducted, and the results were compared and analyzed to preliminarily assess the potential benefits of adding drive units to the chain transmission system.

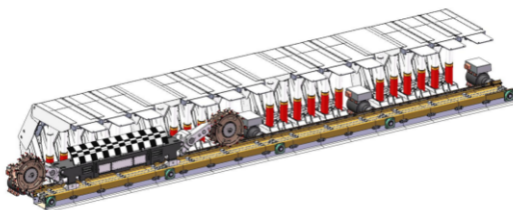


Figure 1. Model of Multi-Point Drive Scraper Conveyor

2. Dynamic Simulation Analysis of the Chain Drive System in Scraper Conveyors

2.1. Establishment of the Dynamic Model for Chain Drive Systems

The research focuses on the SGZ1200/2100 model scraper conveyor. A simulation model was created using Solidworks, and after assembly in Solidworks to ensure there were no interferences, the model was saved as a Parasolid (*.x_t) format file. This file was then imported into ADAMS to obtain the simulation models depicted in Figure 2 and Figure 3.

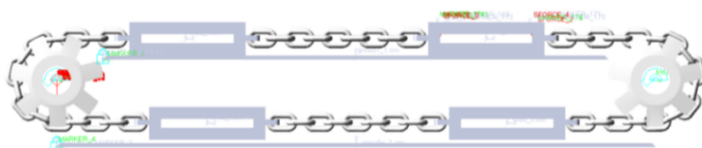


Figure 2. Simulation of the Dual-Motor Chain Drive System



Figure 3. Simulation of the Triple-Motor Chain Drive System

In a multi-motor drive setup, the reduced wrap angle between the middle sprocket and the chain can lead to unstable engagement, resulting in the potential for chain jumping. To address this issue, it's essential to install a chain-tightening device to ensure a secure connection between the middle sprocket and the chain. In Figure 3, the red square represents a pressure plate that simulates this chain-tightening structure.

In both models, the dimensional parameters of sprockets, round-link chains, and load equivalent models are identical. The key difference between dual-drive and multi-point drive systems lies in their approach. In traditional dual-drive chain transmission systems, additional drive points are strategically added based on load characteristics to reduce stress on the chains and tail sprockets.

2.2. Configuration of Simulation Parameters

Gravity was set to act along the negative Y-axis with a magnitude of 9.8 m/s^2 . To represent the motors within the sprocket drive system, they were simplified as equivalent driving torques applied to the sprockets. Material properties were assigned to the components of the chain drive system, with the sprockets made from 23MnCrNiMo material and the circular link chains constructed from 30CrMnSiNi material. Contact force parameters were defined according to Table 1, where $k = 2 \times 10^7 \text{ N/m}$, $c = 500 \text{ N} \cdot \text{s/mm}$, static friction coefficient was set at 0.3, and dynamic friction coefficient was set to 0.1.

Table 1. Contact Force Parameter Settings

Label	Setting	Label	Setting
Normal Force	Collision	Friction Force	Coulomb
Force Exponent	1.5	Static Friction Coefficient	0.3
Damping	500	Dynamic Friction Coefficient	0.1
Stiffness	2.0×10^7	Static Translational Velocity	1×10^{-4}
Penetration Index	0.01	Dynamic Translational Velocity	1×10^{-3}

The running resistance on the loaded side between adjacent sprockets, denoted as (f_l), is determined by the force analysis and is given by:

$$f_l = (q\mu_m + q_0\mu_l)Lg \cos \beta \pm (q + q_0)Lg \sin \beta \quad (1)$$

The running resistance between adjacent sprockets on the empty side (f_k) is given by:

$$f_k = (\mu_l \cos \beta \mp \sin \beta)q_0Lg \quad (2)$$

In the formula, (q_0) and (q) represent the unit length mass of the chain and transported coal, in kg/m ; (β) is the inclination angle of the scraper conveyor, in degrees; (L) is the distance between adjacent chain wheels of the designed scraper conveyor, in meters; (μ_m) and (μ_l) are the resistance coefficients of coal and scraper chain in the middle trough; '+' is taken for upward operation, and '-' for downward operation.

During the operation of the scraper conveyor, as the hydraulic cylinder pushes the body of the scraper conveyor toward the coal wall, the scraper conveyor is subjected to

bending resistance and additional resistance. The calculation of resistance is complex, and according to literature, it is generally calculated based on approximately 10% of the sum of the resistances at the loaded end and unloaded end. Therefore, the total operating resistance (F_z) is given by:

$$F_z = k_1(f_l + f_k) \quad (3)$$

In the equation, (k_1) represents the coefficient for the bending running resistance and additional resistance of the scraper conveyor. Here, it is assumed to be 1.1.

In accordance with the specified parameters for the SGZ1200/2100 scraper conveyor, a rotational speed of 0.86 radians per second is introduced to the rotating mechanism between the sprocket and the ground. Based on research findings and design guidelines^[8], we assume a resistance coefficient of 0.45 for coal material within the central trough, and a resistance coefficient of 0.3 for the scraper chain within the same trough. The mass per unit length (q_0) of the scraper chain is 80 kg/m. Calculations reveal that the mass per unit length of coal material when fully loaded (q) is approximately 534 kg/m. The installation angle (β) is set at 0 degrees, and the acceleration due to gravity (g) is considered as 9.8 m/s².

With these design parameters and length considerations, we can compute the basic operational resistances for the loaded and unloaded ends of the scraper conveyor. When fully loaded, the resistance (f_l) is determined to be 777,042 N, and when unloaded, the resistance (f_k) is 70,560 N. Consequently, the total operational resistance for the scraper conveyor (F_z) is found to be 847,062 N.

Loading conditions are classified into two scenarios. In the first scenario, during unloaded operation, no additional load is applied to either the scraper or the load equivalent model. In the second scenario, during fully loaded operation, with a simulated design length of 5 m and considering the calculated parameters, a force of 105,950.25 N is applied to each of the two scrapers and the load equivalent model at the loaded end.

2.3. Analysis of Simulation Results

For the simulation, a time span of 0.5 seconds was set with a total of 100 simulation steps. Once the simulation solving phase concluded, we proceeded to the post-processing stage. In this stage, torque diagrams for the sprockets were generated under both unloaded and fully loaded conditions, and these are illustrated in Figures 4, 5, 6, and 7.

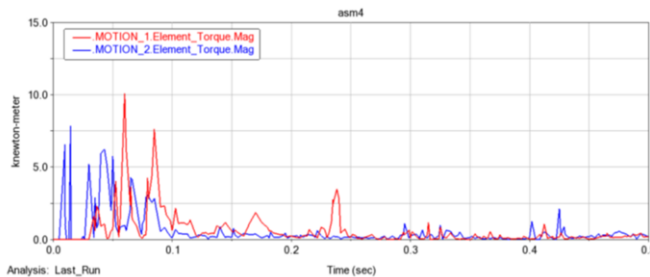


Figure 4. Torque Diagrams for Each Motor in Dual-Drive System under Unloaded Conditions

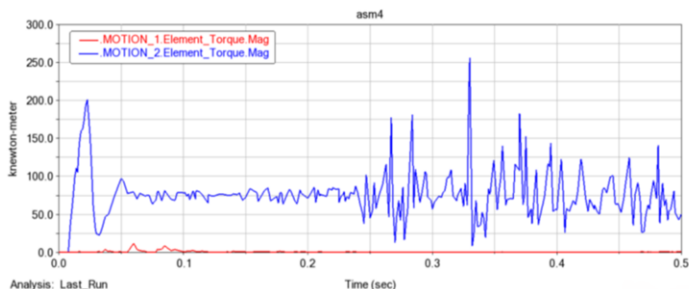


Figure 5. Torque Diagrams for Each Motor in Dual-Drive System under Fully Loaded Conditions

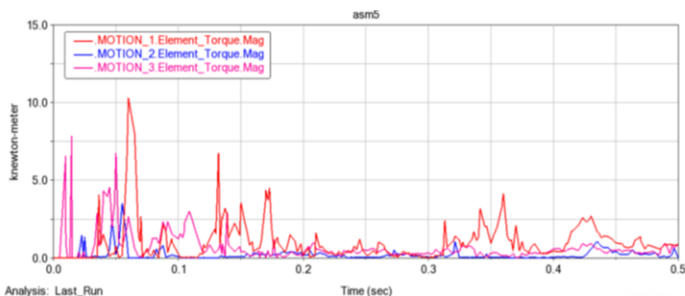


Figure 6. Torque Diagrams for Each Motor in Triple-Drive System under Unloaded Conditions

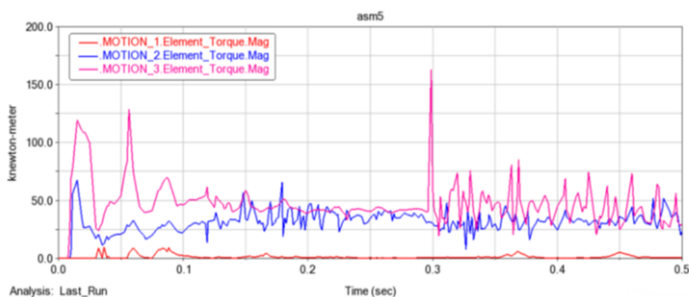


Figure 7. Torque Diagrams for Each Motor in Triple-Drive System under Fully Loaded Conditions

In Figures 4 and 5, "motion1" corresponds to the head motor, while "motion2" represents the tail motor. In Figures 6 and 7, "motion1" stands for the head motor, "motion2" for the middle motor, and "motion3" for the tail motor.

Since we have abrupt torque changes in the setup, our analysis of the simulation results commences after 0.1 seconds, which is when the motor torque stabilizes.

Looking at the torque diagrams in Figures 4 and 5, we notice that in the dual-motor drive system under unloaded conditions, the head and tail motors carry roughly equal torque. However, under full load, the tail motor bears significantly higher torque, averaging about 75 kN • m. This situation can lead to motor overload and uneven sprocket wear, which is detrimental to the long-term stability of the equipment.

Analyzing the torque diagrams in Figures 6 and 7 for the triple-motor drive system under unloaded conditions, we see that all three motors share torque almost equally. Under full load, the head motor still carries lower torque, with the middle motor averaging around 30 kN • m, and the tail motor averaging around 40 kN • m in torque.

3. Conclusion

Based on the simulation results, it is evident that under identical parameter conditions, the torque difference between the front and rear motors in a dual-motor drive system is approximately $75 \text{ kN} \cdot \text{m}$. In contrast, in a triple-motor drive configuration, the torque difference between the front and middle motor is about $30 \text{ kN} \cdot \text{m}$, while the difference between the middle motor and the rear motor is approximately $10 \text{ kN} \cdot \text{m}$. Transitioning from a dual-drive to a triple-drive system indeed improves the load distribution on the rear motor and sprockets, while reducing torque disparities between adjacent motors. This transition effectively mitigates torque imbalances between neighboring motors and lightens the load on the rear motor.

In summary, the incorporation of multi-point drive systems into scraper conveyors holds immense promise for advancing their mechanical and drive technologies, ultimately bolstering the reliability of coal mining equipment. This transition anticipates a future in underground mining marked by heightened safety, increased intelligence, improved efficiency, and enhanced environmental sustainability.

References

- [1] M. Dolipski, E. Remiorz and P. Sobota, "Dynamics of non-uniformity loads of AFC drives", Arch. Mining Sci., vol. 59, no. 1, pp. 155-168, Mar. 2014.A.N. Author, Article title, *Journal Title* **66** (1993), 856–890.
- [2] M. Dolipski, E. Remiorz and P. Sobota, "Follow-up chain tension in an armoured face conveyor", Arch. Mining Sci., vol. 60, no. 1, pp. 25-38, 2015.
- [3] M. Dolipski, E. Remiorz and P. Sobota, "Determination of dynamic loads of sprocket drum teeth and seats by means of a mathematical model of the longwall conveyor", Arch. Mining Sci., vol. 57, no. 4, pp. 1101-1119, 2012.
- [4] K. Herbuś and K. Szewerda, "Analysis of load unevenness of chain conveyor's driving motors on the basis of numerical simulations", J. Achievements Mater. Manuf. Eng., vol. 73, no. 2, pp. 165-175, 2015.
- [5] M. Dolipski, E. Remiorz and P. Sobota, "Follow-up chain tension in an armoured face conveyor", Arch. Mining Sci., vol. 60, no. 1, pp. 25-38, 2015.
- [6] M. Dolipski, E. Remiorz and P. Sobota, "Determination of dynamic loads of sprocket drum teeth and seats by means of a mathematical model of the longwall conveyor", Arch. Mining Sci., vol. 57, no. 4, pp. 1101-1119, 2012.
- [7] Jiang S, Lv R, Wan L, et al. Dynamic characteristics of the chain drive system of scraper conveyor based on the speed difference[J]. IEEE Access, 2020, 8: 168650-168658.
- [8] X. Zhang, W. Li, Z. Zhu, W. Ren and F. Jiang, "Tension monitoring for the ring chain transmission system using an observer-based tension distribution estimation method", Adv. Mech. Eng., vol. 9, no. 9, pp. 1-16, Sep. 2017.
- [9] C. Suvanjumrat, W. Suwannahong and S. Thongkom, "Implementation of multi-body dynamics simulation for the conveyor chain drive system", 3rd Int. Conf. Mechatronics Mech. Eng, Oct. 23, 2016.
- [10] X. Wang, B. Li, S. Wang, Z. Yang and L. Cai, "The transporting efficiency and mechanical behavior analysis of scraper conveyor", Proc. Inst. Mech. Eng. C J. Mech. Eng. Sci., vol. 232, no. 18, pp. 3315-3324, Sep. 2018.